Modified Green–Lindsay model on the reflection and propagation of thermoelastic plane waves at an isothermal stress-free surface

Nihar Sarkar, Soumen De & Nantu Sarkar

Indian Journal of Physics

ISSN 0973-1458

Indian J Phys
DOI 10.1007/s12648-019-01566-9

Springer

Your article is protected by copyright and all rights are held exclusively by Indian Association for the Cultivation of Science. This e-offprint is for personal use only and shall not be self-archived in electronic repositories. If you wish to self-archive your article, please use the accepted manuscript version for posting on your own website. You may further deposit the accepted manuscript version in any repository, provided it is only made publicly available 12 months after official publication or later and provided acknowledgement is given to the original source of publication and a link is inserted to the published article on Springer's website. The link must be accompanied by the following text: "The final publication is available at link.springer.com".

Author's personal copy

Indian J Phys
https://doi.org/10.1007/s12648-019-01566-9

ORIGINAL PAPER

Modified Green–Lindsay model on the reflection and propagation of thermoelastic plane waves at an isothermal stress-free surface

N Sarkar[1], S De[2] and N Sarkar[2]*

[1]Department of Mathematics, City College, Kolkata 700009, India

[2]Department of Applied Mathematics, University of Calcutta, Kolkata 700009, India

Received: 11 March 2019 / Accepted: 06 June 2019

Abstract: The present study is concerned with the reflection and propagation of thermoelastic harmonic plane waves from the stress-free and isothermal surface of a homogeneous, isotropic thermally conducting elastic half-space in the frame of the modified Green–Lindasy (MGL) theory of generalized thermoelasticity with strain rate proposed by Yu et al. (Meccanica 53:2543–2554, 2018). The thermoelastic coupling effect creates two types of coupled longitudinal waves which are dispersive as well as exhibit attenuation. Different from the thermoelastic coupling effect, there also exists one independent vertically shear-type (SV-type) wave. In contrast to the classical Green–Lindsay (GL) and Lord–Shulman (LS) theories of generalized thermoelasticity, the SV-type wave is not only dispersive in nature but also experiences attenuation. Analytical expressions for the amplitude ratios of the reflected thermoelastic waves are determined when a coupled longitudinal wave is made incident on the free surface. The paper concludes with the numerical results on the phase speeds and the amplitude ratios for specific parameter choices. Various graphs have been plotted to analyze the behavior of these quantities. The characteristics of employing the MGL model are discussed by comparing the numerical results obtained for the present model with those obtained in case of the GL and LS models.

Keywords: Generalized thermoelasticity; Modified GL model; Dispersion relation; Attenuation; Reflection

PACS Nos.: 44.10.+i; 46.40.Ff; 62.20.Dc; 91.30.-f; 91.30.Cd

1. Introduction

In the last five decades, thermoelasticity models in which thermal signals propagate at finite velocity were arisen much attention. The classical coupled thermoelasticity (CTE) model proposed by Biot [1] with the introduction of the strain rate term in the Fourier's heat conduction law leads to a diffusion-type heat conduction model. In this model, although the elastic wave propagates with finite phase speed, thermal wave propagates at an infinite phase speed, which is not possible physically. In order to solve this issue, in 1967, Lord and Shulman [2] proposed a generalized thermoelastic model (LS model) based on the Maxwell-Cattaneo [3] model on Fourier's law of heat conduction. After the notable work of Lord and Shulman, Green and Lindsay [4] added temperature rate among the constitutive variables and developed another model (GL model), labeled as temperature rate-dependent generalized thermoelasticity or generalized thermoelasticity with two relaxation times. Both of these theories predict finite speed of propagation of the elastic as well as the thermal wave. There are some engineering materials such as metals which possess a relatively high rate of thermal damping and thus are not suitable for experimental purpose. Due to recent advances in material engineering, the foreseeable future to identify (or even manufacture for laboratory purposes) an idealized material for the purpose of studying the propagation of thermal waves at finite speed is possible. In the beginning of 1990s, the relevant theoretical developments on the subject have been done by Green and Naghdi (GN) [5–7]. They provided sufficient primary modifications in the constitutive relations those permit to deal with a wider class of heat flow problems, entitled as GN I, GN II and GN III. Among these three types of models, the linearized form of GN I is the same as the classical thermoelasticity

*Corresponding author, E-mail: nsarkarindian@gmail.com

Published online: 13 July 2019

© 2019 IACS

Author's personal copy

theory based on the classical Fourier's heat conduction law. On the contrary, the linearized forms of GN II and GN III models permit the finite speed of propagation of thermal signals. The entropy flux vector in GN II and GN III theory was modeled in terms of the potential that also influences stresses. The GN theory II does not contain dissipation of thermal energy in contrast to the GN theory of type III which is considered as thermoelasticity theory with energy dissipation. Other remarkable works based on the above theories of generalized thermoelasticity can be found in the studies [8–16].

Following the notable work of Green and Lindsay [4], recently, Yu et al. [20] established a new model of generalized thermoelasticity theoretically by considering the strain rate term in the Green–Lindsay (GL) model [4] of generalized thermoelasticity with the aid of extended thermodynamics. A problem of semi-infinite one-dimensional thermoelastic medium with traction-free at one end and subjected to a temperature rise using the Laplace transform method is also studied by Yu et al. [20]. They observed that the strain rate may eliminate the discontinuity of the displacement at the elastic and thermal wave fronts. They compared the present model [20] with the Green–Naghdi (GN) models [6, 7] and conclude that the thermal wave speed of the present model is faster than the GN II model [7] and slower than the GN III model [6]. They also showed that their new model is free from the jump discontinuity occurred in the displacement distribution in case of GL model, and is safer in engineering practices than GN model. Later, Quintanilla [21] reported some qualitative results for the modified Green–Lindsay (MGL) thermoelasticity [20]. He proved the exponential decay of the solutions and given a description of the spatial behavior of the solutions of the modified Green–Lindsay thermoelasticity. He also deduced a result on the continuous dependence of the solutions with respect to the initial conditions and to the supply terms and established the exponential stability of the solutions with respect to the time in the case where the supply terms vanish.

The study of propagation of seismic waves in thermoelastic media is of great importance in various fields such as earthquakes, geophysics, soil dynamics and seismology. Wave phenomenon in a thermoelastic medium is of great practical importance in various technological and geophysical circumstances. The propagation of waves along with other geophysical and geothermal data carries information about the structure and distribution of underground magnum. The wave propagation as part of exploration seismology helps in various economic activities like tracing of hydrocarbons and other mineral ores which are essential for various developmental activities like construction of dams, huge buildings, roads, bridges, the design of highways as well as foundation problems in soil mechanics. The problem of reflection of plane waves has been the subject of several investigations. Some of the notable work on waves in thermoelastic media is listed in the studies [22–30]. Reflection of coupled generalized temperature rate-dependent thermoelastic waves on a half-space was investigated by Gupta et al. [31]. Abo-Dahab [32] discussed the propagation of P-, T- and SV-waves at the interface between two solid–liquid media with magnetic field and initial stress in the context of two thermoelastic theory. Biswas and Sarkar [33] derived the solution of the steady oscillations equations in porous thermoelastic medium with dual-phase-lag model. They also studied the phase velocity, attenuation coefficient and penetration depth of time-harmonic plane waves in porous thermoelastic medium with dual phase lag. Li et al. [34] investigated the reflection and transmission of elastic waves at an interface with consideration of couple stress and thermal wave effects. Recently, Sarkar and Tomar [35] reported plane waves in nonlocal thermoelastic solid with voids and Mondal and Sarkar [36] studied waves in dual-phase-lag thermoelastic materials with voids based on Eringen's nonlocal elasticity. Das et al. [37] discussed the reflection of plane waves from the stress-free isothermal and insulated boundaries of a nonlocal thermoelastic solid. Lotfy et al. [38] investigated the thermomechanical response model on a reflection photothermal diffusion waves for semiconductor medium.

During our literature review, we noticed that no thermoelastic plane wave reflection problem has been studied so far in the context of the new modified Green–Lindasy theory [20]. In the present investigation, we study the reflection phenomenon of thermoelastic plane harmonic waves from the isothermal stress-free surface of a homogeneous, isotropic thermally conducting solid half-space by employing the MGL theory of generalized thermoelasticity with strain rate, proposed by Yu et al. [20]. The thermoelastic coupling effect creates two types of coupled longitudinal waves which are dispersive as well as exhibit attenuation. Different from the thermoelastic coupling effect, there also exists one independent vertically shear-type (SV-type) wave. In contrast to the classical Green–Lindsay (GL) and Lord–Shulman (LS) theories of generalized thermoelasticity, the SV-type wave is not only dispersive in nature but also experiences attenuation. Analytical expressions for the amplitude ratios and their respective energy ratios for reflected thermoelastic waves are determined when a coupled longitudinal wave is made incident on the free surface. The paper concludes with the numerical results on the phase speeds, amplitude ratios and their respective energy ratios for specific parameter choices. Various graphs have been plotted to analyze the behavior of these quantities. The characteristics of employing the MGL model are discussed by comparing the

Author's personal copy

numerical results obtained for the present model with those obtained in case of the GL [4] and LS [2] theories of thermoelasticity.

2. Basic governing equations

A thermoelastic process is a coupled dynamical process of an exchange of mechanical energy into thermal energy and vice versa under the action of externally applied thermo-mechanical loading. Such a process is accompanied by strain and temperature changes inside the continuum, all of which vanish upon the removal of the applied loading. The process can be described in terms of the physical field variables like temperature, displacement vector and strain tensor. In the present study, we consider the modified Green–Lindsay (MGL) model [20] to investigate the reflection and propagation of thermoelastic plane waves from the isothermal stress-free surface of a homogeneous, isotropic thermally conducting solid half-space. Following [20], the basic equations of the MGL model for a homogeneous, isotropic thermally conducting elastic medium (in the absence of heat supply and body force) can be arranged in the following way (in general Cartesian coordinates system $Oxyz$):

$$\left(1+\tau_1\frac{\partial}{\partial t}\right)\left[\mu u_{i,jj}+(\lambda+\mu)u_{j,ij}\right]-\gamma\left(1+\tau_1\frac{\partial}{\partial t}\right)\Theta_{,i}=\rho\ddot{u}_i, \tag{1}$$

$$K_T\Theta_{,ii}=\rho C_{\mathrm{E}}\left(1+\tau_0\frac{\partial}{\partial t}\right)\dot{\Theta}+\gamma T_0\left(1+\tau_0\frac{\partial}{\partial t}\right)\dot{e}_{ss}, \tag{2}$$

$$\sigma_{ij}=\left(1+\tau_1\frac{\partial}{\partial t}\right)\left(2\mu e_{ij}+\lambda e_{kk}\delta_{ij}\right)-\gamma\left(\Theta+\tau_1\dot{\Theta}\right)\delta_{ij}. \tag{3}$$

In the above equations, u_i are the displacement components, $e_{ij}=(u_{i,j}+u_{j,i})/2$ are the components of the elastic strain tensor, $e_{kk}(=u_{k,k})$ is the dilatation, σ_{ij} are the components of the elastic stress tensor, t is the time, λ, μ are Lamé constants, $\gamma=(3\lambda+2\mu)\alpha_T$ is the thermoelastic coupling parameter, α_T is the coefficient of linear thermal expansion, ρ is the mass density, C_{E} is the specific heat at constant strain, Θ is the thermodynamic temperature above the reference temperature T_0 such that $|\Theta/T_0|\ll 1$, τ_0, τ_1 are the thermal relaxation parameters such that $\tau_1\geq\tau_0\geq 0$, K_T is the thermal conductivity of the material and $i,j=x,y,z$.

In order to study the present problem in the context of three generalized thermoelasticity models, namely MGL, GL and LS models, we now write the unified form of Eqs. (1)–(3) as

$$\left(1+t_0\tau_1\frac{\partial}{\partial t}\right)\left[\mu u_{i,jj}+(\lambda+\mu)u_{j,ij}\right]-\gamma\left(1+t_1\tau_1\frac{\partial}{\partial t}\right)\Theta_{,i}=\rho\ddot{u}_i, \tag{4}$$

$$K_T\Theta_{,ii}=\rho C_{\mathrm{E}}\left(1+\tau_0\frac{\partial}{\partial t}\right)\dot{\Theta}+\gamma T_0\left(1+t_2\tau_0\frac{\partial}{\partial t}\right)\dot{e}_{ss}, \tag{5}$$

$$\sigma_{ij}=\left(1+t_0\tau_1\frac{\partial}{\partial t}\right)\left(2\mu e_{ij}+\lambda e_{kk}\delta_{ij}\right)-\gamma\left(\Theta+t_1\tau_1\dot{\Theta}\right)\delta_{ij}, \tag{6}$$

where t_0, t_1, t_2 are some constant parameters used to write the above equations under the three models in a unified way. Equations (4)–(6) reduce to the particular set of equations for the MGL, GL and LS models, when

- *MGL model* $t_0=t_1=t_2=1$.
- *GL model* $t_0=t_2=0, t_1=1$.
- *LS model* $t_0=t_1=0, t_2=1$.

3. Formulation of the problem

We consider a linear, homogeneous, isotropic thermally conducting elastic half-space, $z\geq 0$ at uniform reference temperature T_0 as shown in Fig. 1. Let the origin O of the fixed rectangular Cartesian coordinate system $Oxyz$ be fixed at a point on the plane boundary $z=0$ with positive z-axis pointing vertically downward into Ω and x-axis is directed along the horizontal direction. The y-axis is taken in the direction of the line of intersection of the plane wave front with the plane surface. The boundary surface $z=0$ is assumed to be isothermal and free from the mechanical stresses.

If we restrict our analysis to the plane strain problem parallel to the x–z plane, then all the field variables may be taken as functions of x, z and t only. Hence, the displacement components and the temperature field are of the form

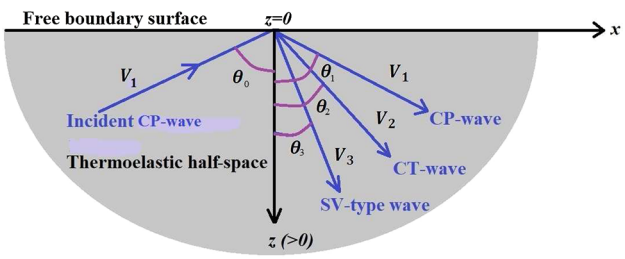

Fig. 1 Schematic of the present problem: incident and reflected thermoelastic waves at the surface $z=0$

Author's personal copy

$$u_1 = u(x,z,t), u_2 = v(x,z,t) = 0, \\ u_3 = w(x,z,t), \Theta = \Theta(x,z,t). \tag{7}$$

Also, in order to obtain the dimensionless forms of Eqs. (4)–(6) under the above assumptions, we introduce the following variables

$$(x',z') = C_L\eta(x,z), (u',w') \\ = C_L\eta(u,w), (t',\tau_0',\tau_1') = C_L^2\eta(t,\tau_0,\tau_1), \\ \Theta' = \frac{\gamma\Theta}{\rho C_L^2}, \sigma_{ij}' = \frac{\sigma_{ij}}{\rho C_L^2},$$

where $C_L^2 = (\lambda+2\mu)/\rho$ is the speed of classical longitudinal (dilatational) wave and $\eta = \rho C_E/K_T$ is the thermal viscosity.

Equations (4)–(6) are then simplified to the following dimensionless forms:

$$\left(1+t_0\tau_1\frac{\partial}{\partial t}\right)\left[\beta^2\left(\frac{\partial^2 u}{\partial x^2}+\frac{\partial^2 u}{\partial z^2}\right)+(1-\beta^2)\frac{\partial e}{\partial x}\right] \\ -\left(1+t_1\tau_1\frac{\partial}{\partial t}\right)\frac{\partial\Theta}{\partial x} = \frac{\partial^2 u}{\partial t^2}, \tag{8}$$

$$\left(1+t_0\tau_1\frac{\partial}{\partial t}\right)\left[\beta^2\left(\frac{\partial^2 w}{\partial x^2}+\frac{\partial^2 w}{\partial z^2}\right)+(1-\beta^2)\frac{\partial e}{\partial z}\right] \\ -\left(1+t_1\tau_1\frac{\partial}{\partial t}\right)\frac{\partial\Theta}{\partial z} = \frac{\partial^2 u}{\partial t^2}, \tag{9}$$

$$\frac{\partial^2\Theta}{\partial x^2}+\frac{\partial^2\Theta}{\partial z^2} = \left(1+\tau_0\frac{\partial}{\partial t}\right)\frac{\partial\Theta}{\partial t}+\varepsilon_\Theta\left(1+t_2\tau_0\frac{\partial}{\partial t}\right)\frac{\partial e}{\partial t}, \tag{10}$$

$$\sigma_{xx} = \left(1+t_0\tau_1\frac{\partial}{\partial t}\right)\left[2\beta^2\frac{\partial u}{\partial x}+(1-2\beta^2)e\right]-\left(1+t_1\tau_1\frac{\partial}{\partial t}\right)\Theta, \tag{11}$$

$$\sigma_{zz} = \left(1+t_0\tau_1\frac{\partial}{\partial t}\right)\left[2\beta^2\frac{\partial w}{\partial z}+(1-2\beta^2)e\right]-\left(1+t_1\tau_1\frac{\partial}{\partial t}\right)\Theta, \tag{12}$$

$$\sigma_{xz} = \beta^2\left(1+t_0\tau_1\frac{\partial}{\partial t}\right)\left(\frac{\partial u}{\partial z}+\frac{\partial w}{\partial x}\right), \tag{13}$$

where $\beta = \sqrt{\mu/(\lambda+2\mu)} = C_S/C_L$ is the ratio of the classical shear wave speed (C_S) to the classical longitudinal wave speed (C_L) and $\varepsilon_\Theta = \gamma^2 T_0/[\rho C_E(\lambda+2\mu)]$ is the dimensionless thermoelastic coupling constant.

We now introduce the displacement potentials ϕ and ψ through the Helmholtz vector representation as

$$u = \frac{\partial\phi}{\partial x}-\frac{\partial\psi}{\partial z}, w = \frac{\partial\phi}{\partial z}+\frac{\partial\psi}{\partial x}. \tag{14}$$

Substituting (14) in Eqs. (8)–(10), we obtain

$$\left(1+t_0\tau_1\frac{\partial}{\partial t}\right)\left(\frac{\partial^2\phi}{\partial x^2}+\frac{\partial^2\phi}{\partial z^2}\right)-\frac{\partial^2\phi}{\partial t^2} \\ -\left(1+t_1\tau_1\frac{\partial}{\partial t}\right)\Theta = 0, \tag{15}$$

$$\beta^2\left(1+t_0\tau_1\frac{\partial}{\partial t}\right)\left(\frac{\partial^2\psi}{\partial x^2}+\frac{\partial^2\psi}{\partial z^2}\right)-\frac{\partial^2\psi}{\partial t^2} = 0, \tag{16}$$

$$\frac{\partial^2\Theta}{\partial x^2}+\frac{\partial^2\Theta}{\partial z^2} = \left(1+\tau_0\frac{\partial}{\partial t}\right)\frac{\partial\Theta}{\partial t} \\ +\varepsilon_\Theta\left(1+t_2\tau_0\frac{\partial}{\partial t}\right)\frac{\partial}{\partial t}(\nabla^2\phi). \tag{17}$$

Equations (15) and (17) show that the thermal field Θ is coupled with the displacement potential ϕ and thus generate two sets of coupled longitudinal waves, namely a coupled longitudinal elastic wave (CP-wave) and a coupled thermal wave (CT-wave). On the other hand, Eq. (16) creates one independent modified vertically shear-type wave (SV-type wave) which is not affected by the presence of the thermal wave as reported in [23–26].

4. Dispersion equation and its solutions

For harmonic plane wave propagating in the direction where the wave normal vector lies in the x-z plane making an angle θ_0 with the positive z-axis (see Fig. 1), the solutions of Eqs. (15)–(17) can be assumed as

$$(\phi,\Theta,\psi) = (\phi^0,\Theta^0,\psi^0) \\ \exp\{\iota k(x\sin\theta_0 - z\cos\theta_0)-\iota\omega t\}, \tag{18}$$

where ϕ^0,Θ^0,ψ^0 are the constants (possible complex) representing the coefficients of the wave amplitudes, $\iota = \sqrt{-1}$, k is the (dimensionless) complex wavenumber and $\omega(>0)$ is the (dimensionless) assigned angular frequency.

If we set, $k = \Re(k)+\iota\Im(k)$, where $\Re(\cdot)$ and $\Im(\cdot)$ denote the real and imaginary parts, it may be verified that for the waves to be physically realistic, we should have $\Re(k)>0$ and $\Im(k)\geq 0$ and that only the real parts of the solutions in (18) are physically relevant [39]. Then, for these waves, $\omega/\Re(k)$ is the phase speed and $\Im(k)$ is the decay (attenuation) coefficient.

Inserting (18) into Eqs. (15)–(17), we obtain the following system of linear algebraic equations for the unknowns ϕ^0,Θ^0 and ψ^0:

$$\left[(1-\iota\tau_1\omega t_0)k^2-\omega^2\right]\phi^0+(1-\iota\tau_1\omega t_1)\Theta^0 = 0, \tag{19}$$

$$\left[\beta^2(1-\iota\tau_1\omega t_0)k^2-\omega^2\right]\psi^0 = 0, \tag{20}$$

Author's personal copy

$$\iota\varepsilon_\Theta\omega(1-\iota\tau_0\omega t_2)k^2\phi^0+\left[k^2-\iota\omega(1-\iota\tau_0\omega)\right]\Theta^0=0. \tag{21}$$

The condition for the existence of non-trivial solutions for ϕ^0 and Θ^0 of the system of Eqs. (19) and (21) yields the following dispersion equation

$$\begin{aligned}&\left[(1-\iota\tau_1\omega t_0)k^2-\omega^2\right]\left[k^2-\iota\omega(1-\iota\tau_0\omega)\right]\\&\quad-\iota\varepsilon_\Theta\omega(1-\iota\tau_0\omega t_2)(1-\iota\tau_1\omega t_1)k^2=0.\end{aligned} \tag{22}$$

4.1. Discussion of the dispersion relation

- *MGL model* If $t_0=t_1=t_2=1$, Eq. (22) reduces to

$$\begin{aligned}&\left[(1-\iota\tau_1\omega)k^2-\omega^2\right]\left[k^2-\iota\omega(1-\iota\tau_0\omega)\right]\\&\quad-\iota\varepsilon_\Theta\omega(1-\iota\tau_0\omega)(1-\iota\tau_1\omega)k^2=0,\end{aligned} \tag{23}$$

which is the dispersion equation of the coupled dilatational elastic and thermal waves in the frame of MGL model [20].

- *GL model* If $t_0=t_2=0, t_1=1$, then Eq. (22) becomes

$$\begin{aligned}&\left[k^2-\omega^2\right]\left[k^2-\iota\omega(1-\iota\tau_0\omega)\right]\\&\quad-\iota\varepsilon_\Theta\omega(1-\iota\tau_1\omega)k^2=0.\end{aligned} \tag{24}$$

Equation (24) is the dispersion equation of the coupled dilatational elastic and thermal waves under the GL model [4] as reported by Agarwal [25]. Again, for $\tau_1=\tau_0=\tau$, Eq. (24) agrees with the result of Nayef and Nemat-Nasser [23].

- *LS model* For $t_0=t_1=0, t_2=1$, Eq. (22) reduces to

$$\begin{aligned}&\left[k^2-\omega^2\right]\left[k^2-\iota\omega(1-\iota\tau_0\omega)\right]\\&\quad-\iota\varepsilon_\Theta\omega(1-\iota\tau_0\omega)k^2=0.\end{aligned} \tag{25}$$

Equation (25) is the dispersion equation of the coupled dilatational elastic and thermal waves in the LS theory [2] as obtained by Puri [24] and Nayef and Nemat-Nasser [23].

- *CTE model* If we substitute $\tau_0=\tau_1=0$, then the dispersion relation (22) reduces to

$$k^4-k^2\left[\omega^2+\iota\omega(1+\varepsilon_\Theta)\right]+\iota\omega^3=0, \tag{26}$$

which is the dispersion relation for the propagation of plane waves in case of CTE model, earlier discussed by Chadwick and Sneddon [22].

So, we conclude that Eq. (22) represents the more general dispersion relation for the coupled longitudinal thermoelastic waves in the frame of the MGL, GL, LS and CTE models in a unified way. For given ω, Eq. (22) gives us four roots, namely $\pm k_1$ and $\pm k_2$, for k. Of these four roots, only two roots yield positive values for $\Re(k)$ along with $\Im(k_{1,2})\geq 0$. Hence, there are two possible distinct traveling coupled dilatational thermal-elastic waves of wavenumbers k_1 and k_2, namely a CP-wave and a CT-wave. These coupled waves are influenced by the strain rate present in the MGL model. The phase speeds of the CP- and CT-waves are given by, $V_{1,2}=\omega/\Re(k_{1,2})$ [43]. Since the attenuation coefficients $\Im(k_{1,2})$ and the phase speeds $V_{1,2}$ are nonlinear functions of ω, which in turn means that the CP-wave and the CT-wave exhibit attenuation as well as dispersion due to the thermoelastic character of the medium in question. The material properties of the medium and the strain rate term of the MGL model influence the dispersion and the attenuation nature of these waves. Besides, since the wavenumbers of these waves are complex, so they are inhomogeneous waves.

Equation (22), for $\varepsilon_\Theta=0$ admits the solutions

$$k_1^2=\frac{\omega^2}{(1-\iota\tau_1\omega t_0)}, k_2^2=\iota\omega(1-\iota\tau_0\omega). \tag{27}$$

Hence, for $\varepsilon_\Theta\neq 0$, we may then call k_1 and k_2, the wavenumber of CP- and CT-waves, respectively, by following Agarwal [40], Roy Choudhuri [41] and Sharma et al. [42]. Consequently, for the present problem, we conclude that V_1 and V_2 are the phase speeds of the CP-wave and the CT-wave, respectively, both of which are modified by the presence of the thermal relaxation times and the strain rate of the MGL model.

The CP- and the CT-waves are coupled dilatational thermal-elastic waves and the coupling is measured by the following amplitudes ratios:

$$\left(\frac{\Theta^0}{\phi^0}\right)_j=\frac{\omega^2-(1-\iota\tau_1\omega t_0)k_j^2}{(1-\iota\tau_1\omega t_1)}=\zeta_j(j=1,2). \tag{28}$$

Equation (20) is the secular equation for the SV-type wave. A look at Eq. (20) reveals that this wave propagates with the phase speed V_3 given by

$$V_3=\frac{\omega}{\Re(k_3)}, k_3=\frac{\omega}{\beta\sqrt{1-\iota\tau_1\omega t_0}}. \tag{29}$$

The expressions in (29) show that the SV-type wave is affected by the presence of the strain rate of the MGL model, while the thermal field has no influence on this wave. It is also interested to note that this wave is not only dispersive in nature but also attenuated in contrast to the GL, LS and CTE models (see [22–26] for details).

5. Reflection problem

Let a train of CP-wave having amplitude A_0 and phase speed V_1 is made incident making an angle θ_0 with the normal to the free surface $z=0$, as shown in Fig. 1. Assuming the radiation in vacuum is neglected, when it impinges the boundary $z=0$, three types of reflected waves (CP-, CT- and SV-type) in the medium in question are created. Suppose the reflected CP-, CT- and SV-type waves make angles θ_1, θ_2 and θ_3, respectively, with the

Author's personal copy

positive z-axis. Then, the complete structures of the wave fields consisting of the incident and reflected waves in the medium may be expressed as

$$\phi = A_0 \exp\{\iota k_1(x\sin\theta_0 - z\cos\theta_0) - \iota\omega t\} + \sum_{j=1}^{2} A_j \exp\{\iota k_j(x\sin\theta_j + z\cos\theta_j) - \iota\omega t\}, \tag{30}$$

$$\Theta = \zeta_1 A_0 \exp\{\iota k_1(x\sin\theta_0 - z\cos\theta_0) - \iota\omega t\} + \sum_{j=1}^{2} \zeta_j A_j \exp\{\iota k_j(x\sin\theta_j + z\cos\theta_j) - \iota\omega t\}, \tag{31}$$

$$\psi = B_1 \exp\{\iota k_3(x\sin\theta_3 + z\cos\theta_3) - \iota\omega t\}, \tag{32}$$

where A_1, A_2 and B_1 represent the coefficients of amplitudes of the reflected CP-, CT- and SV-type waves, respectively. The amplitude ratios are defined as the amplitude ratios of the reflected waves to the incident wave and are determined by the well-defined boundary conditions at $z = 0$.

Let us now consider the surface $z = 0$ to be isothermal and stress-free. Mathematically, these conditions may be written in non-dimensional forms as

$$\sigma_{zz} = \sigma_{xz} = \Theta = 0, \text{at} z = 0. \tag{33}$$

In terms of displacement potential functions, the first two conditions in (33) can be written as

$$\left(1 + \tau_1 t_0 \frac{\partial}{\partial t}\right)\left(\frac{\partial^2\phi}{\partial z^2} + \frac{\partial^2\phi}{\partial x^2}\right) + 2\beta^2\left(1 + \tau_1 t_0 \frac{\partial}{\partial t}\right)\left(\frac{\partial^2\psi}{\partial x \partial z} - \frac{\partial^2\phi}{\partial x^2}\right) - \left(1 + \tau_1 t_1 \frac{\partial}{\partial t}\right)\Theta = 0, \tag{34}$$

$$\left(2\frac{\partial^2\phi}{\partial x \partial z} + \frac{\partial^2\psi}{\partial x^2} - \frac{\partial^2\psi}{\partial z^2}\right) = 0, \text{ at } z = 0. \tag{35}$$

In order to satisfy the above boundary conditions at $z = 0$, the angles of the reflected waves must be related with the angle of the incident CP-wave by the following relation:

$$k_1 \sin\theta_0 = k_1 \sin\theta_1 = k_2 \sin\theta_2 = k_3 \sin\theta_3. \tag{36}$$

Relation (36) can also be written as

$$\theta_0 = \theta_1 \text{ and } \frac{\sin\theta_0}{V_1} = \frac{\sin\theta_2}{V_2} = \frac{\sin\theta_3}{V_3}. \tag{37}$$

Substituting from Eqs. (30)–(32) into (33)–(35) and using the relation (36), the following system of equations for the amplitude ratios $R_{CP} = A_1/A_0, R_{CT} = A_2/A_0$ and $R_{SV} = B_1/A_0$ is obtained:

$$\begin{bmatrix} a_{11} & a_{12} & a_{13} \\ a_{21} & a_{22} & a_{23} \\ \zeta_1 & \zeta_2 & 0 \end{bmatrix} \begin{bmatrix} R_{CP} \\ R_{CT} \\ R_{SV} \end{bmatrix} = \begin{bmatrix} -a_{11} \\ a_{21} \\ -\zeta_1 \end{bmatrix}, \tag{38}$$

where

$$a_{11} = \omega^2 - 2\beta^2(1 - \iota\tau_1\omega t_0)k_1^2 \sin^2\theta_0,$$
$$a_{12} = \omega^2 - 2\beta^2(1 - \iota\tau_1\omega t_0)k_2^2 \sin^2\theta_2, a_{13} = \omega^2 \sin 2\theta_3,$$
$$a_{21} = k_1^2 \sin 2\theta_0, a_{22} = k_2^2 \sin 2\theta_2, a_{23} = -k_3^2 \cos 2\theta_3.$$

After solving (38), we get the amplitude ratios R_{CP}, R_{CT}, R_{SV} of the reflected CP-, CT- and SV-type waves, respectively, in explicit forms. It is observed that the amplitude ratios depend on the angle of incidence (θ_0) and the material properties of the thermoelastic medium. It can also be noted that for uncoupled thermoelasticity ($\varepsilon_\Theta = 0$), $\zeta_j = 0 (j = 1, 2)$, and hence, there will be no reflected CT-wave. So, in this case $R_{CT} = 0$ at each angle of incidence θ_0.

6. Results and discussions

With the view of illustrating the analytical results obtained in the previous sections, we now present some numerical results. The material chosen for this purpose is crust, whose material properties are [44]

$$\lambda = \mu = 3.0 \times 10^{10}\text{N m}^{-2}, T_0 = 300\text{K},$$
$$\rho = 2900\text{kgm}^{-3}, C_E = 1100\text{J kg}^{-1}\text{K}^{-1}$$
$$K_T = 3.0\text{W m}^{-1}\text{K}^{-1}, \alpha_T = 1.0667 \times 10^{-5}\text{K}^{-1},$$
$$\varepsilon_\Theta = 0.00268, \tau_0 = 0.25, \tau_1 = 2\tau_0, \omega = 0.2.$$

MATLAB R2010a software on a personal computer is used for the purpose of numerical computations.

In Fig. 2a–c, the comparisons for the amplitude ratios of the reflected CP-, CT- and SV-type waves with respect to the angle of incidence θ_0 ($0° \le \theta_0 \le 90°$) of the incident CP-wave have been shown in case of the three models: the MGL, GL and LS models of generalized thermoelasticity. Figure 3a and b reveals that the amplitude ratios $|R_{CP}|$, and $|R_{CT}|$ are largest for MGL model when compared to the GL and LS models within the whole range of θ_0. Figure 3c shows that the amplitude ratio $|R_{SV}|$ of the reflected SV-type wave is remaining greater in MGL model within $0° \le \theta_0 \le 60°$ only, and within the range $60° < \theta_0 \le 90°$, it remains lesser in MGL when compared to GL and LS models. Each of the amplitude ratio attains their maximum at $\theta_0 = 90°$ for all the three models.

In Fig. 3a–c, we studied how the relaxation time parameter τ_1 affects the variation of the amplitude ratios $|R_{CP}|$, $|R_{CT}|$, and $|R_{SV}|$ under the MGL model when the other relaxation time parameter τ_0 is kept fixed, namely

Author's personal copy

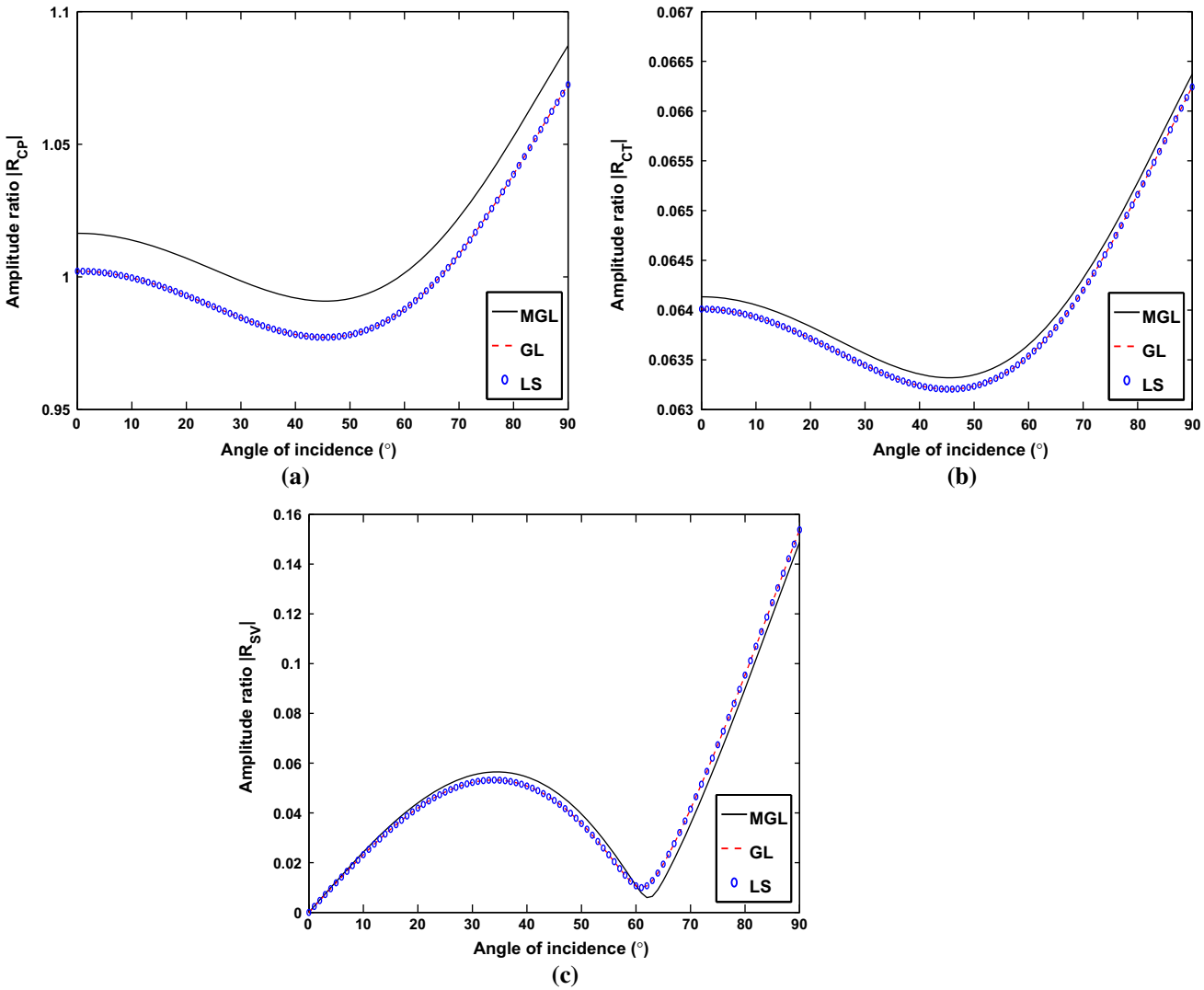

Fig. 2 Variations of (**a**) $|R_{CP}|$, (**b**) $|R_{CT}|$ and (**c**) $|R_{SV}|$ with θ_0 for incident CP-wave under four models

$\tau_0 = 0.25$. In calculations, four different values of τ_1, that is, $\tau_1 = \tau_0, 2\tau_0, 3\tau_0$ and $4\tau_0$ are considered. Figure 3a and c exhibits that the amplitude ratios $|R_{CP}|$ and $|R_{SV}|$ increase gradually with the increase of τ_1. On the contrary, in Fig. 3b, we observed that the amplitude ratio $|R_{SV}|$ decreases as τ_1 increases for $0^\circ \leq \theta_0 \leq 60^\circ$. It is also evident that the amplitude ratios $|R_{CP}|$, and $|R_{CT}|$ are most sensitive to the relaxation time parameter τ_1, while the amplitude ratio $|R_{SV}|$ is only sensitive to τ_1 only in the range $0^\circ \leq \theta_0 \leq 68^\circ$, approximately.

The effect of the Poisson's ratio (σ) on the behavior of the amplitude ratios are also interesting. In Fig. 4a–c, we investigated how the Poisson's ratio affects the amplitude ratios $|R_{CP}|$, $|R_{CT}|$ and $|R_{SV}|$ under the MGL model. In the calculations, four different values of the σ, namely $\sigma = 0.25, 0.30, 0.33, 0.36$, are taken. The Poisson's ratio has an increasing effect on amplitude ratios $|R_{CP}|$ and $|R_{CT}|$ within the range $0^\circ \leq \theta_0 \leq 65^\circ$ and decreasing effect within rest of the range of θ_0. On the contrary, σ has an decreasing effect on $|R_{SV}|$ for the whole range of the angle of incidence θ_0. It is also noticed that the all the amplitude ratios are affected significantly by the Poisson's ratio.

Figure 5a and b reveals the influence of the thermoelastic coupling parameter ε_Θ on the phase speeds of CP-wave (V_1) and CT-wave (V_2), respectively, with respect to the dimensionless angular frequency ω in case of the MGL model. The phase speeds are calculated for $\varepsilon_\Theta = 0.0, 0.00268, 0.00536$, and 0.00804. It is clear that ε_Θ has significant impact on V_1, and V_2. Both of the phase speeds decrease gradually as ε_Θ increases, which in turn means that ε_Θ has decreasing effect on the phase speeds of the CP- and CT-waves. We also observed that for a fixed ε_Θ, the phase speed V_1 first increases gradually within the range $10 \leq \omega \leq 20$and then decreases sharply for $20 < \omega \leq 100$. On the hand, Fig. 5b shows that the phase speed V_2 increases rapidly for the range $10 \leq \omega \leq 30$, and thereafter

Author's personal copy

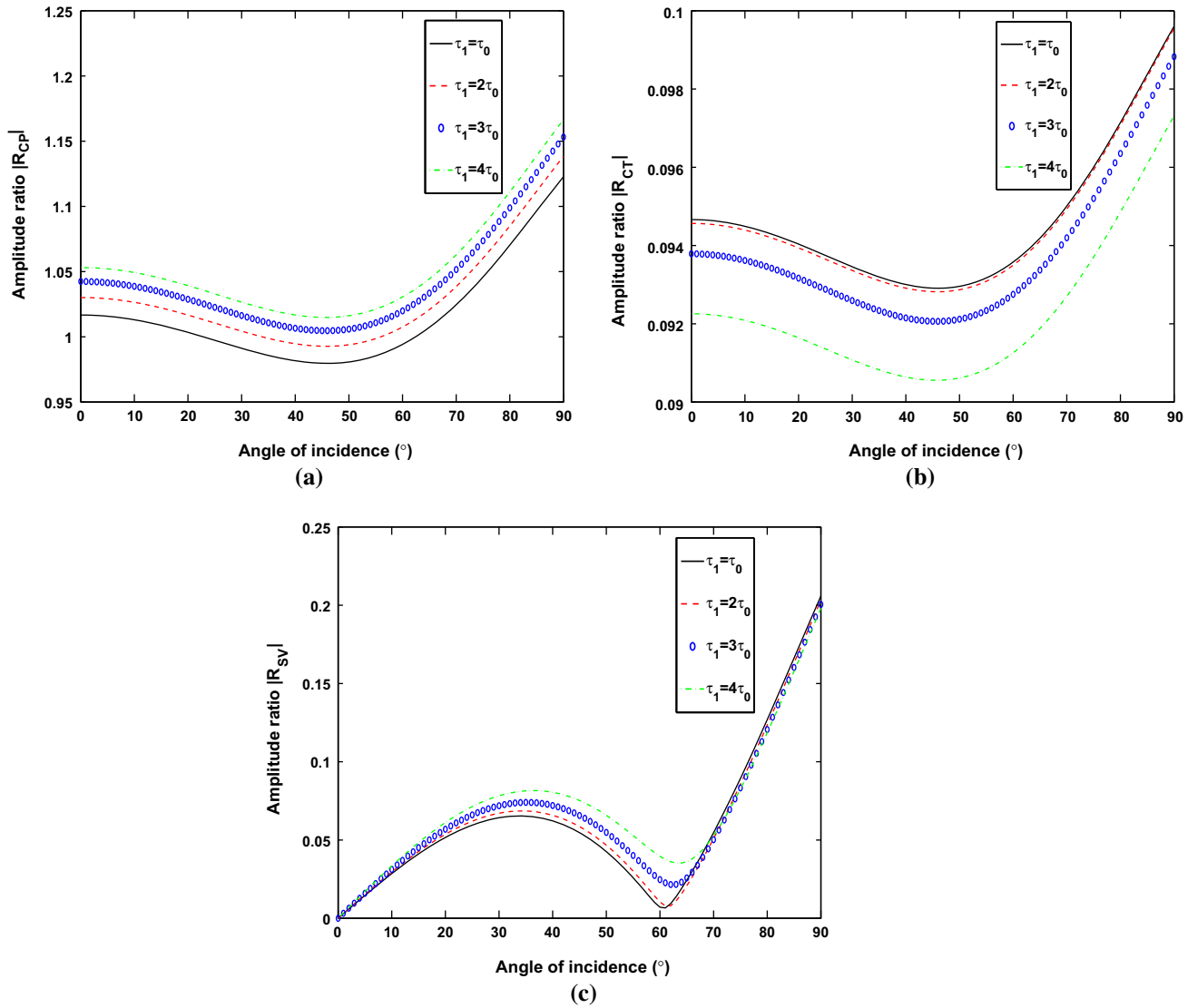

Fig. 3 Variation of (**a**) $|R_{CP}|$, (**b**) $|R_{CT}|$ and (**c**) $|R_{SV}|$ with θ_0 for incident CP-wave at various values of τ_1 for fixed $\tau_0 = 0.25$ under MGL model

it becomes steady for $\omega > 30$. These graphs expressed that the CP- and CT-waves are dispersive in nature, which is the verification of a result already pointed out in the text. As we have also pointed out in the text that the SV-type wave remaining unaffected by the presence of the thermal field, here we did not present the variation of the SV-wave speed for various ε_Θ.

In Fig. 6a and b, we presented the variations of the phase speeds V_1 and V_2 versus ω for various values of the relaxation time parameter τ_1 while keeping the other relaxation time parameter τ_0 fixed, namely $\tau_0 = 0.25$. These figures expressed that the relaxation time parameter τ_1 has significant influences the variations of the phase speeds V_1 and V_2. Both of the phase speeds are decreasing as the relaxation time parameter τ_1 increases. Figures 5 and 6 depict that the CP-wave is the slowest, while the CT-wave wave is the fastest one within the whole range of ω $(10 \leq \omega \leq 100)$.

At last, Fig. 7 is drawn to compare our numerical result for the phase speed of the CP-wave obtained in case of CTE model with the result presented in Fig. 1 earlier by Chadwick and Sneddon in their notable work [22]. We noticed that, for the CTE theory $(\tau_0 = \tau_1 = 0)$, the variation of the phase speed of the CP-wave in Fig. 7 is completely agree with Fig. 1 in [22].

7. Conclusions

In a thermoelastic medium under the MGL theory, there are totally three kinds of propagating waves. The thermoelastic coupling generates two sets of coupled

Author's personal copy

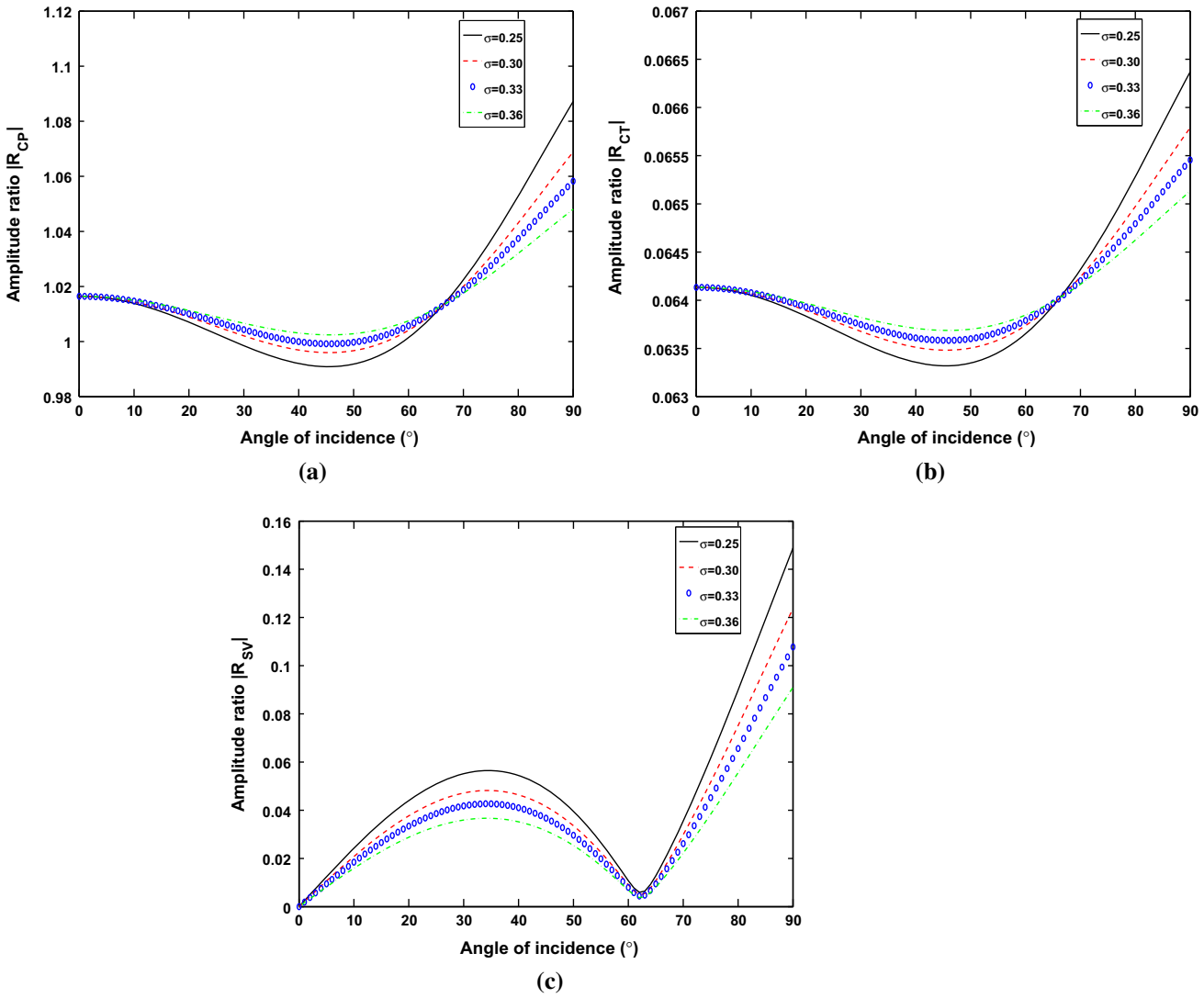

Fig. 4 Variation of (**a**) $|R_{CP}|$, (**b**) $|R_{CT}|$ and (**c**) $|R_{SV}|$ with θ_0 for incident CP-wave at various values of Poisson's ratio σ under MGL model

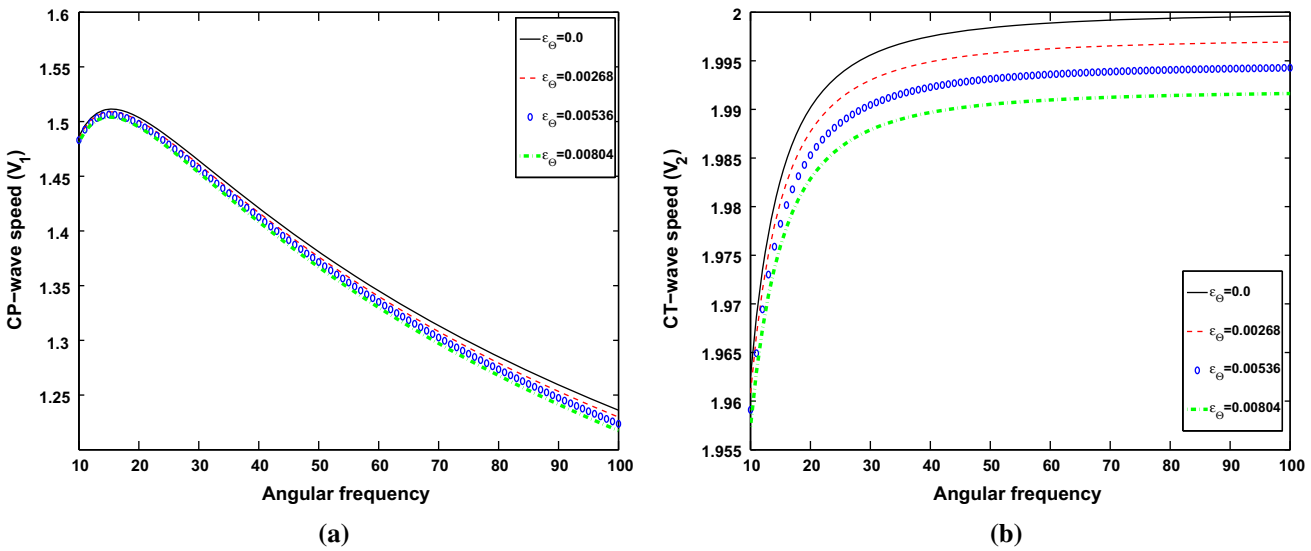

Fig. 5 Variation of the phase speeds (**a**) V_1 and (**b**) V_2 with angular frequency ω for various values of ε_Θ under MGL model

Author's personal copy

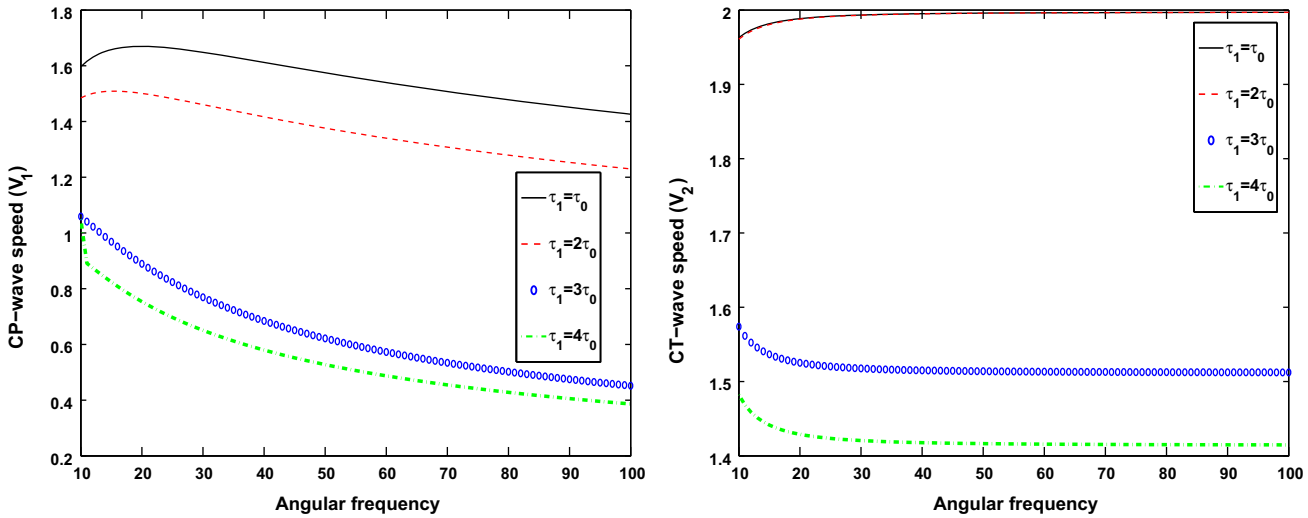

Fig. 6 Variation of the phase speeds (**a**) V_1 and (**b**) V_2 with ω for various values of τ_1 for fixed $\tau_0 = 0.25$ under MGL model

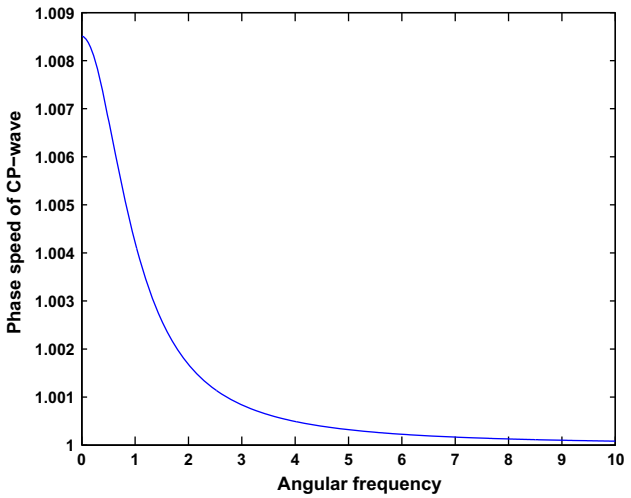

Fig. 7 The phase speed of CP-wave versus angular frequency for CTE model

longitudinal waves. There is also one independent SV-type wave. The reflection of thermoelastic waves is also studied for the incident CP-wave at a stress-free isothermal surface. The thermal field affects only the longitudinal waves. The coupling between the displacement and the temperature fields makes the longitudinal waves (CP- and CT-waves) not only dispersive but also attenuated. Similarly, the introduction of the MGL model makes the SV-type wave not only dispersive but also attenuated, in contrast to the other generalized thermoelastic models. Numerical results show that the amplitude ratios and of the reflected CP-, CT- and SV-type waves are significantly affected by the relaxation time parameter τ_1 as well as the Poisson's ratio. It is also observed that the maximum amount of the incident wave is reflected as (reflected) CP-wave. The phase speed of the CP-wave as well as the CT-wave is sensitive to ε_Θ, while the phase speed of SV-type wave is insensitive to ε_Θ. The phase speed of the SV-type wave depends on the Poisson's ratio only. The present theoretical and numerical results may provide interesting and significant information for experimental scientists, researchers and seismologists working on this type of problem.

References

[1] M Biot *J. Appl. Phys.* **27** 240 (1956)
[2] H W Lord and Y Shulman *J. Mech. Phys. Solids* **15** 299 (1967)
[3] C Cattaneo *Comptes. Rendus. Acad. Sci.* **2** 431 (1958)
[4] A E Green and K A Lindsay *J. Elast.* **2** 1 (1972)
[5] A E Green and P M Naghdi *Proc. R. Soc. Lond. A* **432** 171 (1991)
[6] A E Green and P M Naghdi *J. Therm. Stresses* **15** 253 (1992)
[7] A E Green and P M Naghdi *J. Elast.* **31** 189 (1993)
[8] M Marin *Acta Mech* **122** 155 (1997)
[9] H H Sherief, A M A El-Sayed and A M A El-Latief *Int. J. Solids Struct.* **47** 269 (2010)
[10] H M Youssef *J. Heat Trans.* **132** 61301-1 (2010)
[11] Y Z Povstenko *J. Therm. Stresses* **34** 97 (2011)
[12] Y J Yu, W Hu and X-G Tian *Int. j. Eng. Sci.* **81** 123 (2014)
[13] M Bachher, N Sarkar and A Lahiri *Int. J. Mech. Sci.* **89** 84 (2014)
[14] Y J Yu, X-G Tian and Q-L Xion *Eur. J. Mech. A Solids* **60** 238 (2016)
[15] Y J Yu, Z-N Xu, C-L Li and X-G Tian *Compos. Struct.* **146** 108 (2016)
[16] M Marin *Contin. Mech. Thermodyn.* **29** 1365 (2017)
[17] K Lotfy, R Kumar and W Hassan *Appl. Math. Mech. Engl. Ed.* **39** 783 (2018)
[18] K Lotfy *Sci. Rep.* **9** 3319 (2019)
[19] K Lotfy *Wave Random. Complex* (2019) https://doi.org/10.1080/17455030.2019.1580402

Author's personal copy

[20] Y J Yu, Z-N Xue and X-G Tian *Meccanica* **53** 2543–2554 (2018)
[21] R Quintanilla *Meccanica* **53** 3607 (2018)
[22] P Chadwick and I N Sneddon *J. Mech. Phys. Solids* **6** 223 (1958)
[23] A H Nayfeh and S Nemat-Nasser *Acta Mech.* **12** 53 (1971)
[24] P Puri *Int. J. Eng. Sci.* **11** 735 (1973)
[25] V K Agarwal *Acta Mech.* **34** 185 (1979)
[26] S K Roychoudhuri and S Mukhopadhyay *Int. J. Math. Math. Sci.* **23** 497 (2000)
[27] S B Sinha and K A Elsibai *J. Therm. Stresses* **20** 129 (1997)
[28] J N Sharma, V Kumar and D Chand *J. Therm. Stresses* **26** 925 (2003)
[29] M I A Othman and Y Q Song *Acta Mech.* **184** 189 (2006)
[30] M I A Othman and Y Q Song *Int. J. Solids Struct.* **44** 5651 (2007)
[31] N D Gupta, A Lahiri and N C Das *Math. Mech. Solids***17** 543 (2011)
[32] S M Abo-Dahab *Can. J. Phys.* **93** 1 (2015)
[33] S Biswas and N Sarkar *Mech. Mater.* **126** 140 (2018)
[34] Y Li, W Wang, P Wei and C Wang *Meccanica* **53** 2921 (2018)
[35] N Sarkar and S K Tomar *J. Therm. Stresses* **42** 580 (2019)
[36] S Mondal, N Sarkar and N Sarkar *J. Therm. Stresses* **42** 1035 (2019)
[37] N Das, N Sarkar and A Lahiri *Appl. Math. Model.* **73** 526 (2019)
[38] K Lotfy, S M Abo-Dahab and R Tantawy *Silicon* (2019) https://doi.org/10.1007/s12633-019-00116-6
[39] D S Chandrasekharaiah *Mech. Res. Commun.* **23** 549 (1996)
[40] V K Agarwal *Acta Mech.* **34** 181 (1979)
[41] S K Roychoudhuri *J. Elast.* **15** 59 (1985)
[42] J N Sharma, D Grover and D Kaur *Appl. Math. Model.* **35** 3396 (2011)
[43] J D Achenbach *Wave Propagation in Elastic Solids* (New York: North-Holland) (1976)
[44] M C Singh and N Chakraborty *Appl. Math. Model.* **37** 463 (2013)

Publisher's Note Springer Nature remains neutral with regard to jurisdictional claims in published maps and institutional affiliations.